J. Exp. Biol. (1967), **46**, 431–443
With 8 *text-figures*
Printed in Great Britain

FLIGHT IN *DROSOPHILA*

III. AERODYNAMIC CHARACTERISTICS OF FLY WINGS AND WING MODELS

By STEVEN VOGEL

*Biological Laboratories, Harvard University, Cambridge, Massachusetts**

(*Received* 21 *December* 1966)

INTRODUCTION

The preceding paper of this sequence (Vogel, 1967) demonstrated that the wings of fruit-flies operate under conditions unusual even for flapping-wing aircraft. In particular, we noted that the fly does not rigorously maintain a 'preferred' angle of attack, but allows this parameter to vary over a wide range. The present investigation seeks to relate these special operating circumstances to the aerodynamic characteristics of the wings themselves. The literature discloses no previous measurements on lift-producing airfoils at Reynolds numbers around 100. Hence it is also of interest to determine which properties of fly wings reflect specific specializations of that airfoil and which are direct consequences of operation in its dimensional range.

In the flapping flight of insects, the wing, without auxiliary airfoils, must produce both lift and thrust; functions which, in conventional aircraft, are divided between wings and propellers. Consequently, although the present measurements were made on fixed wings, they apply to operating conditions between those encountered by propeller blades and helicopter rotors. Thus the angle of attack and the force components, lift and drag, are expressed, not with respect to an unchanging horizontal plane, but to the instantaneous direction of the relative wind on the wings. The relationship between the lift and drag of an airfoil and the lift and thrust produced by flapping the airfoil has been qualitatively described by Chadwick (1953).

MATERIAL

Wings were cut from female *Drosophila virilis* and used immediately. Models for use in the wind tunnel were made of 0·025 mm. thick 'Mylar' (polyester) magnetic recording tape trimmed to the desired shape. For observation of flow patterns in an analogous liquid system, a rectangular model was cut from 1 mm. thick transparent Perspex.

METHODS

1. *Mounting wings and models for use in the wind tunnel*

Largely because of the complex and non-rigid nature of the wing articulation, the mounting of fly wings presented serious problems. The following procedure, of the many that were tried, gave the least distortion of wing shape during mounting and

* Present address: Department of Zoology, Duke University, Durham, North Carolina 27706.

subsequent measurements. The wing was placed, ventral surface downward, on a microscope slide beneath a cover slip with the wing base protruding beyond the edge of the slide. A 4-mil wire with a drop of 'Tackiwax' (Central Scientific Co.) on its tip was then positioned so that the wire was aligned with the long axis of the wing and its tip made light contact with the wing base. A heated wire loop was brought near enough to melt the wax and bond the wing base to the wire mount. Removal of the cover slip allowed the wing to regain its normal contours. Wing shape was essentially stable for 3–5 hr. after mounting.

Certain wings showed a cambered profile similar to that observed in photographs of the downstroke in tethered flight (Vogel, 1967). These wings are identified as such in the figures and table. It was not possible to alter the camber of mounted wings.

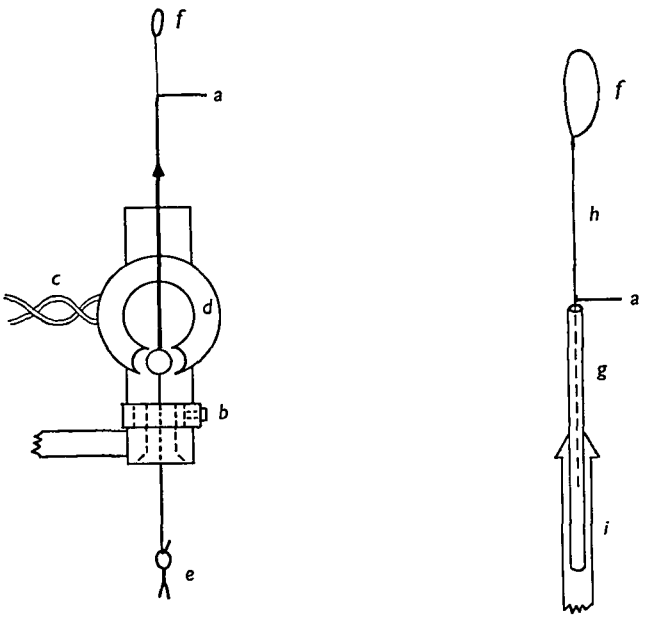

Fig. 1. Apparatus for measuring lift and drag of fly wings and wing models. *a*, lever for changing angle of attack; *b*, set-screw locking orientation of assembly around its vertical axis; *c*, leads from control unit; *d*, galvanometer; *e*, counterweights; *f*, wing or model; *g*, steel tube; *h*, mount-wire; *i*, needle of galvanometer.

Model wings were mounted in a similar manner. Models four times natural size could be cambered easily, if not reproducibly, by gently rolling them around a small shaft, with the long axes of shaft and airfoil parallel.

2. *Polar diagrams*

Measurements of forces on the wings and models were made with a galvanometric force transducer (Vogel & Chapman, 1966). The air velocity in the wind tunnel (Vogel, 1966) was monitored with a hot-bead thermistor anemometer (similar to that described by Roeder, 1966). Fig. 1 illustrates the specific arrangement of the galvanometer. The airfoil could be rotated with respect to the galvanometer by pushing lever *a*; the entire assembly rotated about its vertical axis after loosening set-screw *b*.

The former adjustment changed the angle of attack, and the latter permitted changing from lift measurements (force normal to tunnel axis) to drag measurements (force parallel to the axis). Neither movement altered the location of the wing in the airstream. The current source for the galvanometer was calibrated to read 2·00 dynes at the full-scale setting of its helical potentiometer.

In order to minimize the drag of the mount-wire, wings were positioned close to the edge of the airstream, and the tunnel exit was arranged to produce a sharp velocity gradient at the edge of the working section. Even so a correction for mount-wire drag was necessary; the correction subtracted was the drag of the mount-wire without the wing. Interaction between test object and mount-wire was neglected.

At each setting of tunnel velocity, lift was measured at about eleven different positive angles of attack, drag at about seven angles; in certain cases an additional set of measurements were made at negative angles. Since the exact angles of attack emerged *post hoc* from photographs of the airfoils, the determinations were not made at equal intervals. Moreover, since the galvanometer had to be rotated in order to shift from measurements of lift to measurements of drag, the angles were different in the two cases. All force measurements were expressed in terms of the dimensionless coefficients of lift (C_L) and drag (C_D); inclusion of wing area (one surface) in the definition of these coefficients accomplished, in effect, the reduction of measurements to the dimensions of a standard animal.

For each wing or model, the lift and drag coefficients were plotted separately against the angle of attack; values were read from these graphs at equal intervals of angle of attack. 10° intervals were used with data obtained from fly wings; for the models, where changes were more abrupt, values were read every 5°. Lift coefficients were plotted against drag coefficients (with the angle of attack treated parametrically) to produce polar diagrams.

3. *Flow patterns*

The technique for producing and photographing flow patterns has already been described (Vogel & Feder, 1966). The pictures presented here were made with a model having an 8·5 mm. chord and slightly sharpened leading and trailing edges, but no camber. The support for the model was arranged so that adjustment of the angle of attack did not require removal of the model from the bath.

4. *Angle of onset of stall*

Detection of stall behind an airfoil operating at Reynolds numbers around 100 is simple and unequivocal. Flow photographs show that 'separation' of flow from the upper airfoil surface occurs under the same conditions as the appearance of fluctuating velocities in the wake of equivalent airfoils detectable with the thermistor probe. Similarly, force measurements indicate that stall also appears under these conditions which produce visible separation. Thus the presence of irregular velocities in the wake is a reliable indication that stall is occurring.

5. *Differences from natural conditions*

Conditions in these experiments differed in three principal respects from normal flight. The techniques employed enforced a steady-flow regime rather than continuous and rapid changes of velocity and angle of attack. The angle of attack was constant

along the length of the airfoil, although, as previously noted (Vogel, 1967), this situation should be approximated only during hovering. Except for the photographs of flow patterns, velocity was also constant across the wingspan, again an abnormal condition. As a consequence of these important differences, the results are not necessarily definitive of tethered flight conditions, much less of free flight.

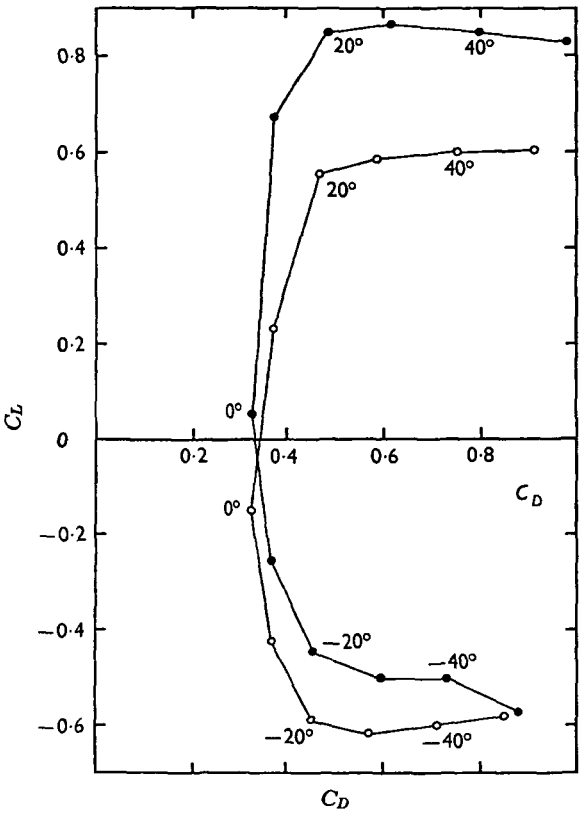

Fig. 2. Polar diagrams for fruit-fly wings at 300 cm./sec., in both flat (○) and cambered (●) configurations. Angle of attack treated parametrically and written on the curves. C_L: coefficient of lift; C_D: coefficient of drag.

RESULTS

1. *Force measurements*

Lift and drag were measured on fruit-fly wings, on rectangular thin plates, and on thin plates of the same outline as fly-wings, in each case at velocities of 100, 200, 300, and 400 cm./sec. Measurements were also made on thin plates shaped like fly wings but with linear dimensions four times larger. These latter models were used at velocities of 50, 75, and 100 cm./sec., and thus were dynamically similar to fly wings at 200, 300, and 400 cm./sec. respectively.

The polar diagrams of the rectangular plates, 1·1 × 3·0 mm. did not differ appreciably from those of plates trimmed to the shape of fly wings. The larger models experienced somewhat less drag than the fly wings or small models, but this probably was due to a relative decrease in the interference of the mounting. In short, there were

no important differences in aerodynamic characteristics among the models, and we need only compare any one model with the fly wings. The larger models will be considered since their camber could be altered.

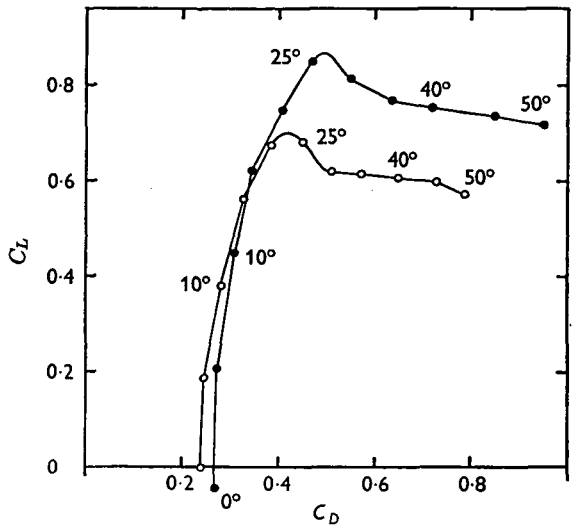

Fig. 3. Polar diagrams for thin plates cut to the shape of fly wings but with linear dimensions four times larger, at 75 cm./sec., in both flat (○) and cambered (●) configurations. C_L: coefficient of lift; C_D: coefficient of drag.

Table 1. *Summary of airfoil performance measurements. Velocities in parentheses are for models four times normal size.* (α = *angle of attack*)

	100 cm./sec.		200 (50)		300 (75)		400 (100)	
Drosophila wing	Flat	Camber	Flat	Camber	Flat	Camber	Flat	Camber
C_D at α = 0	0·520	0·535	0·410	0·425	0·345	0·340	0·295	0·290
L/D max	0·80	1·21	1·00	1·44	1·18	1·87	1·22	1·94
α at L/D max	30°	25°	20°	20°	20°	16°	20°	15°
C_L at L/D max	0·570	0·830	0·525	0·845	0·555	0·785	0·500	0·700
C_D at L/D max	0·710	0·685	0·525	0·585	0·470	0·420	0·410	0·360
C_L max/C_L 50°	1·00	1·29	1·14	1·13	1·00	1·04	1·00	1·01
Thin plates								
C_D at α = 0	—	—	0·320	0·330	0·240	0·265	0·200	0·220
L/D max	—	—	1·61	1·59	1·79	1·81	2·03	2·19
α at L/D max	—	—	21°	24°	20°	25°	19°	19°
C_L at L/D max	—	—	0·755	0·915	0·680	0·850	0·620	0·745
C_D at L/D max	—	—	0·470	0·575	0·380	0·470	0·305	0·340
C_L max/C_L 50°	—	—	1·29	1·27	1·23	1·18	1·14	1·12

Fig. 2 shows the polar diagrams for cambered and uncambered fly wings at 300 cm./sec.; the analogous curves for the large models at their equivalent velocity appear in Fig. 3. Measurements for both wings and models at all velocities are summarized in Table 1. Inspection of these data discloses several noteworthy points:

(1) Camber increased the maximum lift obtainable from both thin plates and fly wings.

(2) Camber was more effective in raising the maximum ratio of lift to drag for fly wings than for thin plates.

(3) Uncambered fly wings performed better at negative than at positive angles of attack: the absolute values of their lift-to-drag ratios were higher for negative angles than for positive angles of the same magnitude at almost all values of velocity and angle of attack.

(4) Lift was more sharply dependent on angle of attack for the thin plates than for the fly wings. The latter maintained nearly maximal lift from 20° to at least 50°.

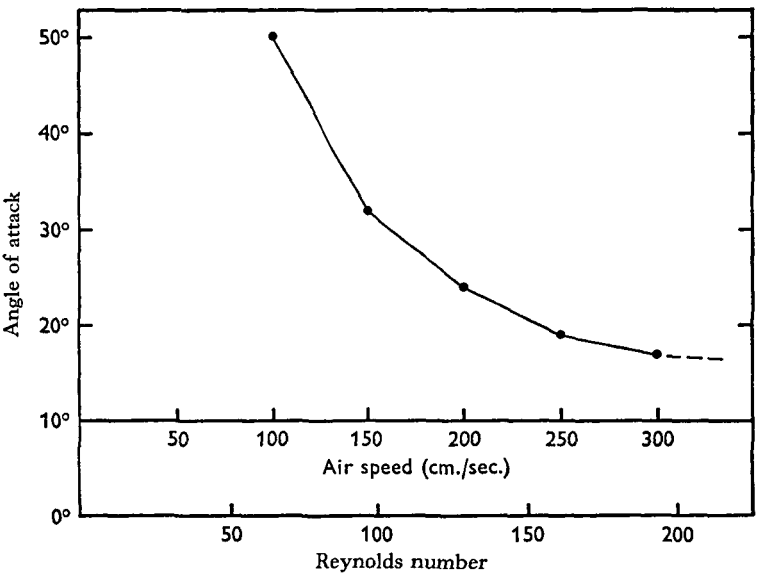

Fig. 4. Angle of onset of stall versus airspeed and Reynolds number for a rectangular flat plate 1·0 mm. wide and of large aspect ratio.

2. *Onset of stall*

The relationship between the onset of stalling and velocity and Reynolds number for a thin plate is illustrated in Fig. 4. As expected, the angle of onset of stall increased as the Reynolds number decreased; the large magnitude of the changes is probably a unique property of this dimensional range. By contrast, irregularities in velocity indicative of stalling could not be detected behind fly wings at angles below 50°; above 50° the results were uncertain. In short, under the experimental conditions the fly wing did not appear subject to stalling at any reasonable velocity or angle of attack.

3. *Flow patterns*

The physical appearance of flow around an airfoil in the dimensional range relevant to flying *Drosophila* is shown in Fig. 5. Stall is concomitant with separation of flow from the upper airfoil surface and results in the formation behind the airfoil of one or two discrete bound vortices. There is no evidence of sustained turbulence or the von Karman trails characteristic of flow around non-streamlined objects at somewhat higher Reynolds numbers. The minimal angle of attack (*c.* 20°) at which stall was

observed in the photographs is similar to the stall angle determined with the micro-anemometer (Fig. 4).

Fig. 6 shows the effect on the flow pattern of lowering the Reynolds number below values at which vortices can be produced. Despite the relative increase in viscous forces the airfoil more effectively deflects the fluid from its original horizontal direction of flow. Clearly, prevention of stall under these conditions, even by lowering the Reynolds number, results in improved performance of an airfoil at high angles of attack.

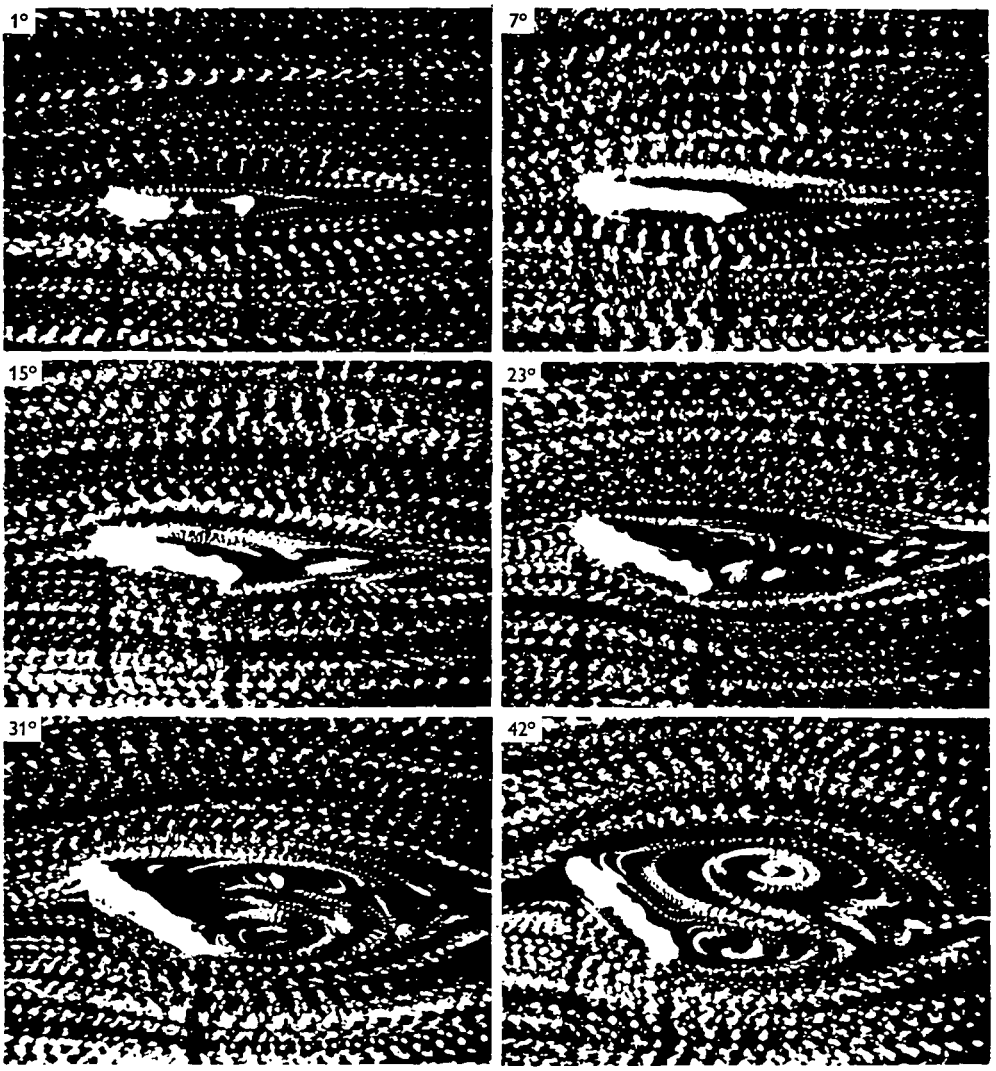

Fig. 5. Flow patterns around a flat plate at a Reynolds number of 120 as the angle of attack is increased in steps from 1° to 42°.

DISCUSSION

1. *Wing camber*

In the dimensional range of fruit-flies, as under more conventional conditions, a slight degree of wing camber considerably increases lift with but a small increase in drag. Since this phenomenon occurs with either fly wings or thin plates, it is probably an intrinsic property of airfoils rather than a result of any morphological specialization of the fly. The superior performance of the cambered airfoils explains the use of a cambered profile by the fruit-fly during down-stroke (Vogel, 1967). These measurements also argue against the involvement of any exotic system for generating lift in these small insects.

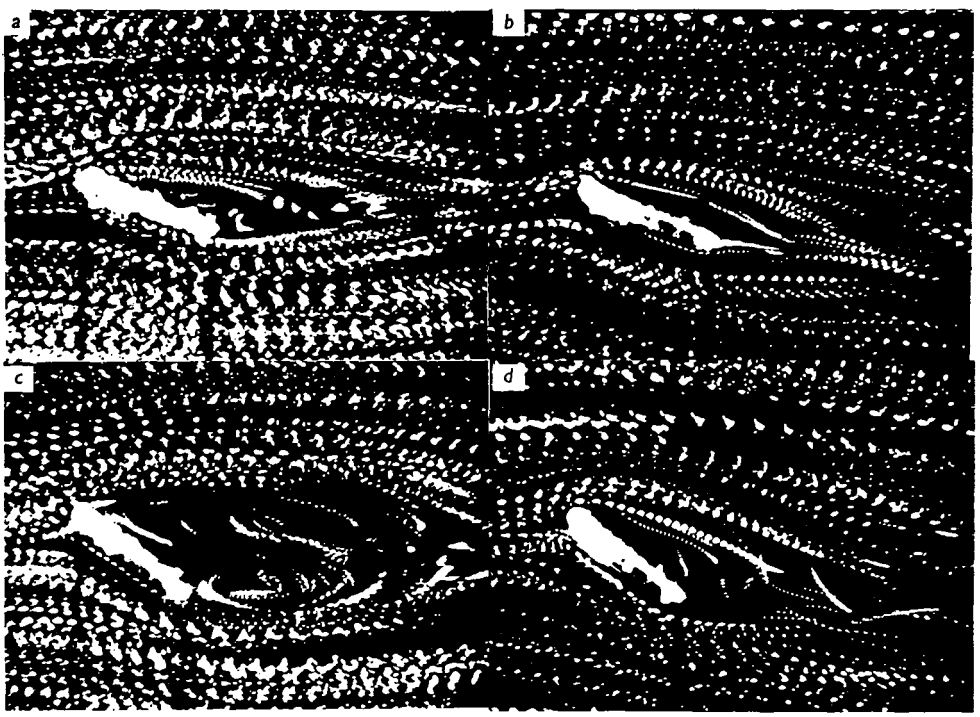

Fig. 6. Flow patterns around a flat plate in relation to angle of attack and Reynolds number. *a* and *b*, angle of attack of 22°; *c* and *d*, 38°. *a* and *c*, Reynolds number of 120; *b* and *d*, 30. Note that flow is deflected further from horizontal in pictures *b* and *d*.

During the upstroke the wing encounters negative angles of attack. As noted earlier (Vogel, 1967), rather than reversing the direction of camber, the fruit-fly simply employs a flat profile during the upstroke. It is therefore significant that flat, uncambered fly wings give greater lift as well as higher lift-to-drag ratios at negative than at positive angles of attack. In addition, this absence of a mirror-image symmetry in performance between negative and positive angles of attack, even in uncambered wings, demonstrates the existence of a functional difference between the upper and lower wing surfaces.

2. *Lift hysteresis near the stall point*

With conventional airfoils it is commonly observed that stall does not immediately follow a sudden increase in the angle of attack to values at which, under conditions of steady flow, stall normally occurs. Instead, for the first few chords of travel, the wing experiences unusually high lift forces (Farren, 1936; Silverstein and Joyner, 1939; Moore, 1956). The present measurements, performed entirely under steady-state conditions, do not indicate whether this 'lift hysteresis' occurs in the fruit-fly's dimensional range or is in any way important to the animal. We may presume that

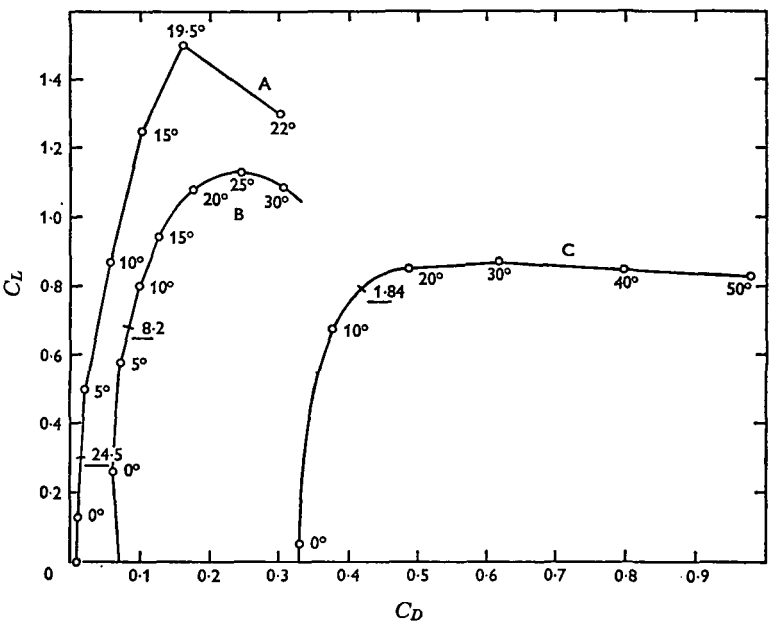

Fig. 7. Polar diagrams for three different airfoils. A. Conventional profile, NACA 2409, aspect ratio of 6, Reynolds number (*Re*) about 5×10^6 (Von Mises, 1945). B. Locust hindwing, *Re* about 4×10^3. C. Fruit-fly wing, *Re* about 2×10^3. On each curve the point of maximum lift-to-drag ratio is marked and the value of the ratio at that point underlined.

lift hysteresis is not important in the flight of fruit-flies, since the design of the fruit-fly wing appears to avoid stalling even in steady flow. Possibly the magnitude of lift hysteresis and the range of angles of attack over which this factor could be effective are insufficient for the demands of the flight of fruit-flies. For a fly travelling at 200 cm./sec., the angle of attack at mid-downstroke must be about 30° greater near the tips of the wings than near their bases. Lift hysteresis over such a wide range would be most remarkable.

3. *Size and wing performance*

Polar diagrams and force coefficients provide a convenient means for comparing the aerodynamic behaviour of wings operating in different dimensional ranges. Fig. 7 presents, on one set of axes, the curves for three successful designs: an airplane wing, the locust hindwing, and the wing of *Drosophila virilis*. In their general performance characteristics the locust and airplane wings are rather similar to each other but differ

strikingly from the fly wing in two principal respects. First, the locust and airplane wings stall at angles of attack greater than about 20°. By contrast, the fly wing shows a broad 'plateau' of high lift extending from about 20° to at least 50°. (The absence of stall will be discussed in section 4, the 'plateau' in section 5.) Secondly, the curve for the fly wing in Fig. 7 is well to the right of those for airplane and locust wings. In short, the fly wing experiences much higher drag forces relative to its size, velocity, and capability for producing lift. The qualitative consequences of this high drag will be briefly described.

As an unavoidable consequence of operation at low Reynolds numbers the fly pays a high price in skin-friction for introducing its wing into the airstream. Relative to this large drag already present at an angle of attack of zero degrees, increasing the angle to produce lift incurs little additional drag. The result is clearly evident in Fig. 7. On each curve the point is marked at which the ratio of lift to drag ('useful' to 'non-useful' force) is maximal. For airplane and locust wings, the lift-to-drag ratio is greatest at $2\frac{1}{2}°$ and 7° respectively—well below the angles of attack where stall could present problems. The fly wing, by contrast, achieves its best performance at an angle of 15°; i.e. very near the point at which stall occurs in equivalent flat-plate models (Figs. 3 and 4).

As noted previously (Vogel, 1967) the fruit-fly employs an untwisted wing. Thus, except in hovering flight, the angle of attack must vary along the length of the wing. Consequently, the fly must operate, not at a particular place on its polar curve, but over a sizeable region of the curve even at a given instant during the stroke. As mentioned earlier, at a forward speed of 200 cm./sec., the angle of attack at mid-downstroke will be about 30° greater near the wing tip than near the base. The fly meets these strange conditions with a wing which resists stalling and whose behaviour is much less dependent on angle of attack than is the case in conventional airfoils. The unusual aerodynamic properties of the wings of fruit-flies, adaptations, as we have seen, to unique operating conditions, are probably unattainable in any other dimensional range.

4. *The structural basis for the absence of stall*

At high angles of attack fruit-fly wings fail to stall whereas thin plates of the same shape stall in a normal fashion. Clearly, the difference in dynamic properties between fly wings and thin plates must be an outcome of their different morphology. The thin plates lack four major features found on the fly wings—the veins and pleating of the wing membrane, the row of hairs along the trailing edge, the large bristles on the leading edge, and the microtrichia which cover the wing surface. It is important to recognize that no single structure need be entirely responsible. Indeed, by analogy with the structural basis for the minimization of body drag (to be published), stall is most probably prevented by the combined effects of several structures. The precise mechanism and structural basis of stall prevention has yet to be determined.

Thick boundary layers characterize flow at low Reynolds numbers. Thus all structures mentioned as possible stall-preventing devices are within the region of low-velocity flow on the surface of the fly wing. Jensen (1956) has suggested that structures within the boundary layer should have little influence on the characteristics of flow across a wing. But, if structures within the boundary layer were unimportant, then the fly wing and wing models should show similar aerodynamic properties. Since this was

not the case, we may tentatively conclude that the nature of flow across a wing under the present conditions may be strongly influenced by events occurring within its boundary layer. Prandtl & Tietjens (1934) state that backflow within a boundary layer leads to vortices and a change in the general pattern of flow.

Several indirect lines of evidence suggest that the microtrichia of the wing surface are at least partly responsible for prevention of stall. Though these small hairs represent a significant fraction of the weight of the wing, they serve no well-documented function. Similar bristles having a different embryological background (macrotrichia) are found on the wings of small wasps. Both micro- and macrotrichia point distally and posteriorly—an orientation which might provide resistance to the reversed flow near the wing surface associated with separation and stall. Since both velocity and angle of attack are maximal near the wing tip, stall should be more of a problem in that area. In addition, separation should first occur near the trailing edge. Significantly, in those species of small flies and wasps which do not have fully bristle-clad wings, bristles are usually retained on the distal and posterior parts of the wing surface.

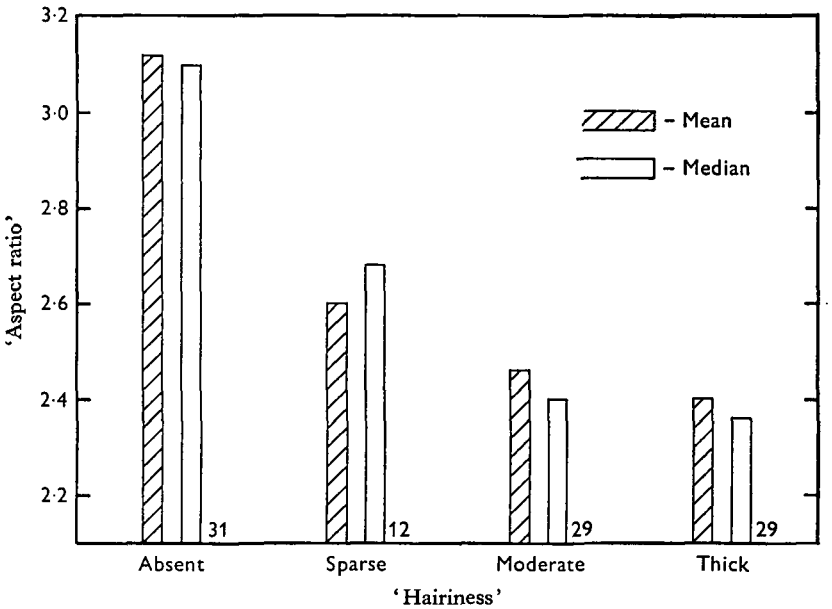

Fig. 8. Length-to-width ratio ('aspect ratio') versus 'hairiness' for the wings of 101 species of Heleidae (*Diptera*). Data from Wirth (1952). Number of species in each category indicated on abscissa.

In order to avoid stall flow must remain 'attached' to the upper airfoil surface for nearly the full transit from leading to trailing edge despite an increasing pressure. Thus the tendency for a stalling vortex to form should increase with the width of the wing, and broad wings should be more subject to stalling than narrow wings. Wirth (1952) has used wing dimensions and the occurrence and extent of surface hairiness as taxonomic characters in a study of biting midges. If one groups his descriptions into appropriate categories, one obtains an inverse relationship between 'hairiness' and the ratio of wing length to width (Fig. 8). If our hypothesis concerning the role

of these short hairs is correct, the species with short, broad wings are better equipped with devices to oppose stall than are those with long, narrow wings.

5. *The interrelationship of lift and drag*

Despite the absence of stall at high angles of attack the lift produced by fly wings is not increased appreciably by increases in the angle of attack above about 20°. Instead, a region of high but relatively constant lift occurs from roughly 20° to at least 50° (Figs. 2 and 7). The existence of this 'plateau' may be explained in the following manner.

By definition, drag is the reduction in momentum flux of a field of flow caused by passage across an obstacle such as an airfoil. Lift is the rate of creation of a downward component of momentum by the airfoil. Thus conditions of high drag may limit the momentum available for deflexion as lift; and lift and drag may be regarded as antagonistic. For conventional airfoils, such as airplane wings, drag is much smaller than lift from very low angles of attack up to the point at which stall begins. Hence any reduction in lift due to drag forces is inconsequential. But for fruit-fly wings, lift and drag are of the same magnitude over most of its polar curve. At high angles of attack any increase in the angular deflexion of the air-stream may be balanced by the concomitant decrease in the rate of flow of air in the wake of the wing (i.e. increasing drag), producing a situation where lift is largely independent of angle of attack. Figs. 6*b* and 6*d* compare the flow around an airfoil at two different angles of attack, stall occurring in neither case. At the higher angle flow in the wake is deflected further from the horizontal by the action of the airfoil. However, the velocities of flow in the wake have suffered a decrease due to the increased drag at the higher angle of attack.

6. *Lift and thrust calculations*

By the use of the polar diagrams and stroke parameters it is possible to calculate the lift and thrust produced by a flapping-wing aircraft. These figures may be compared to the lift and thrust measured on live, performing specimens, as has been done for the desert locust by Jensen (1956). The comparison of calculated and measured performances provides a check on the completeness and adequacy of the data, as well as furnishing some indication as to whether conventional aerodynamic analysis is appropriate for the flapping flight of animals. As yet our data are insufficient to calculate rigorously the performance of fruit-flies; information is lacking on angle of attack and the detailed kinematics of the stroke, and the polar diagrams refer to a situation which differs significantly from that obtaining in normal flight.

Crude calculations have been performed using the stroke data (Vogel, 1966), the information on the variation of angle of attack both with flying speed and along the length of the wing (Vogel, 1967), the present polar diagrams and some guesswork. Two situations were considered: (1) hovering flight, with lift equal to body weight, no thrust, and a horizontal stroke plane; and (2) forward flight at 220 cm./sec., with thrust equal to body drag, no lift, and a vertical stroke plane. In both cases the calculated forces were about one-half of those necessary to sustain flight. In view of the abnormal conditions under which the polar diagrams were obtained and of the uncertainties and simplifications in the computations, the results should not be considered strong evidence of theoretical deficiencies in the analysis. For a machine

designed by the evolutionary process, the only appropriate operating conditions are its natural conditions. Measurements or calculations under other circumstances are more likely to show substandard rather than superior performances.

SUMMARY

1. The variation of the lift and drag of fruit-fly wings with angle of attack and velocity was compared with that of thin plates.

2. High drag and low ratios of lift to drag characterized these airfoils, the primary difference being the absence of stalling in the fly wings.

3. Flow photographs and determinations of stall point on thin plates suggested that the fly wing behaves as if encountering a Reynolds number below the actual value.

4. At positive angles of attack camber improved the aerodynamic characteristics of fly wings; at negative angles uncambered wings were superior.

5. The structural basis for the performance of fly wings and the relationship of their characteristics to their opening conditions are discussed.

REFERENCES

CHADWICK, L. E. (1953). In *Insect Physiology*. Ed. K. D. Roeder. New York: John Wiley and Sons, Inc.; London: Chapman and Hall, Ltd.

FARREN, W. S. (1936). The reaction on a wing whose angle of incidence is changing rapidly. *Rep. aero. Res. Comm. Lond.*, no. 1648, H.M. Stationery Office.

JENSEN, M. (1956). Biology and physics of locust flight. III. The aerodynamics of locust flight. *Phil. Trans.* B **239**, 511–52.

MOORE, F. K. (1956). Lift hysteresis at stall as an unsteady boundary layer phenomenon. *NACA tech. rept.* no. 1291.

PRANDTL, L. & TIETJENS, O. G. (1934). *Applied Hydro- and Aeromechanics*. New York: Dover Publications, Inc. (1957).

ROEDER, K. D. (1966). A differential anemometer for measuring the turning tendency of insects in stationary flight. *Science* **153**, 1634–6.

SILVERSTEIN, A. & JOYNER, U. T. (1939). Experimental verification of the theory of oscillating airfoils. *NACA tech. rept.* no. 673.

VOGEL, S. (1966). Flight in *Drosophila*. I. Flight performance of tethered flies. *J. exp. Biol.* **44**, 567–78.

VOGEL, S. (1967). Flight in *Drosophila*. II. Variations in stroke parameters and wing contour. *J. exp. Biol.* (In the Press.)

VOGEL, S. & CHAPMAN, R. D. (1966). Force measurements using d'Arsonval galvanometers. *Rev. Sci. Instrum.* **37**, 520.

VOGEL, S. & FEDER, N. (1966). Visualization of low-speed flow using suspended plastic particles. *Nature, Lond.* **209**, 186–7.

VON MISES, R. (1945). *Theory of Flight*. New York: Dover Publications, Inc.

WIRTH, W. W. (1952). The Heleidae of California. *Univ. of Calif. Publications in Entomology* **9**, 95–266.